Liquid Crystals
Publication details, including instructions for authors and subscription information:
http://www.informaworld.com/smpp/title~content=t713926090

Molecular modelling of liquid crystal systems: An internal coordinate Monte Carlo approach

Mark R. Wilson[a]
[a] Department of Chemistry, University of Durham, Durham, UK

To cite this Article Wilson, Mark R.(1996) 'Molecular modelling of liquid crystal systems: An internal coordinate Monte Carlo approach', Liquid Crystals, 21: 3, 437 — 447
To link to this Article: DOI: 10.1080/02678299608032852
URL: http://dx.doi.org/10.1080/02678299608032852

LIQUID CRYSTALS, 1996, VOL. 21, NO. 3, 437–447

Molecular modelling of liquid crystal systems: An internal coordinate Monte Carlo approach

by MARK R. WILSON

Department of Chemistry, University of Durham, South Road, Durham DH1 3LE, UK

(*Received 9 August 1995; in final form 27 March 1996; accepted 12 April 1996*)

A Monte Carlo scheme is presented which is designed to provide a convenient mechanism to model accurately the internal molecular structure of liquid crystalline molecules. The technique stores atomic positions in terms of bond lengths, bond angles and dihedral angles within a Z-matrix, and the Monte Carlo scheme involves generating trial configurations from changes to the Z-matrix using the MM2 molecular mechanics potential to describe energy changes between different molecular conformations. The technique is applied to the liquid crystal molecule 4-*n*-pentyl-4′-cyanobiphenyl (5CB), and results are presented for the conformational populations and dihedral angle distributions of 5CB in the gas phase at 300 K. The effect of a nematic mean field on the distribution of molecular conformations is also examined via the addition of a conformation-dependent potential of mean torque to the internal energy.

1. Introduction

The past 10 years have seen the introduction of a range of powerful computational techniques designed to model the structure and properties of simple organic molecules [1, 2]. One of the simplest of these techniques is the molecular mechanics approach [2–5], which attempts to describe molecules by a series of potential functions designed to model each structural feature of a molecule. Usually separate functions exist to describe the distortion of each bond length, bond angle and dihedral angle within a molecule together with each non-bonded interaction between non-adjacent atoms. These functions make up the molecular mechanics *force field*. Each molecular conformation i has a steric energy E_i within the force field which measures how the conformation differs from a hypothetical structure where all structural features have their ideal (or natural) values. E_i has no direct physical significance by itself, but the differences between steric energies of any two conformations is equivalent to the difference in internal energy between them. The structure of any molecule can therefore be optimised by minimizing the value of E_i. This approach is very powerful and a number of molecular mechanics packages exist which are able to carry out fast, efficient minimizations of E_i for a series of trial geometries to provide energy minimized conformations [6, 7]. If required these geometries may be further refined by the use of semi-empirical quantum methods [8]. For small liquid crystal molecules this approach is quite valuable. Molecular mechanics can provide an indication of the lowest energy molecular conformation, and the output coordinates from such a calculation can be used to determine molecular dipoles, polarizabilities, etc. [9]. However, for larger flexible molecules a high number of local minima exist on the energy hypersurface, and this leads to two clear problems with the molecular mechanics approach. Firstly, the large number of available energy minima mean that it is difficult to find the global energy minimum for the system. Secondly, even if a global minimum can be found it is likely that a significant number of molecules will be found in other low lying energy states. If all low-lying energy minima can be found, a Boltzmann weighting can be used to assign fractional populations to each conformation in the calculation of molecular properties. However, this approach is fraught with difficulties, not least because it is always hard to guarantee that all important conformations have been found.

An alternative approach to conformational searching is provided by classical molecular dynamics (MD) and Monte Carlo (MC) methods [10]. Both techniques provide mechanisms to sample conformational space using the same potentials as those derived for molecular mechanics work, providing respectively time-average (MD) and ensemble-average (MC) information about molecular properties. In MD work, Newton's equations of motion are solved using finite difference techniques to integrate the equation of motion, whilst in the Monte Carlo method individual conformations are generated according to a Boltzmann distribution. The MD approach is most closely related to the molecular mechanics method. MM potential functions can be

0267–8292/96 $12·00

differentiated to provide the forces acting on individual atomic sites. However, the MD approach fares rather badly for isolated molecules. Single molecule MD simulations in the temperature range 250–450 K are hampered by the large energy barriers between different conformations, and in practice it is difficult to sample phase space efficiently. Even when newer stochastic MD techniques [11] (specifically aimed to combat this problem) are used, the convergence of average molecular properties is still very slow [12]. Monte Carlo techniques fare equally badly if random changes are made to atomic coordinates in cartesian space. However, the advantage of the MC method is that the sampling of phase space can be carried out through changes to internal coordinates (bond lengths, bond angles and dihedral angles).

The purpose of the current paper is to outline a simple Monte Carlo technique for the simulation of isolated liquid crystal molecules. The technique used stores a generalized set of atomic coordinates in the form of a Z-matrix. Trial Monte Carlo moves are made via changes to the Z-matrix coordinates, with the acceptance or rejection of trial moves based on a Boltzmann factor generated from a standard molecular mechanics potential (MM2). Section 2 of this paper describes the Monte Carlo technique used to model internal molecular structure. In § 3 results are presented for the mesogen 4-*n*-pentyl-4′-cyanobiphenyl (5CB) in the gas phase at 300 K. In §§ 4 and 5 the effect of a nematic field on molecular structure is considered by the introduction of a potential of mean torque which is loosely coupled to the molecular conformation via the inertia tensor. Finally, in § 6 some conclusions are drawn regarding the usefulness of this approach to molecular modelling.

2. Monte Carlo simulations

The Monte Carlo technique used in this work is centred around the use of a Z-matrix to store an internal coordinate representation of a liquid crystal molecule. Z-matrices are well-known in quantum mechanics [1, 13] where they are used to represent molecular structures in terms of bond lengths, bond angles and dihedral angles. In this work we place the further restriction that the dihedral angles used in the Z-matrix are proper dihedrals rather than improper dihedrals which are normally equally valid as input to quantum calculations. The Z-matrix contains a single line for each atom and is described by the following framework which is defined with respect to figure 1

Line 1: defines the name of the atom (atom A) to be placed at the origin.

Line 2: defines the position of the second atom (atom B) in terms of a bond length l_2 from atom A along the x-axis.

Line 3: defines the position of the third atom (atom C) in terms of a bond length l_3 from atom B and a bond angle θ_3 (with atoms A and B) in the x–y plane.

Line 4: defines the position of atom D in terms of the bond length l_4 from atom C, the bond angle θ_4 with atoms B and C, and the dihedral angle ϕ_4 involving atoms A, B, C and D.

Line n: defines the positions of a new atom in terms of a bond length l_n, bond angle θ_n and dihedral angle ϕ_n with respect to three previously defined atoms.

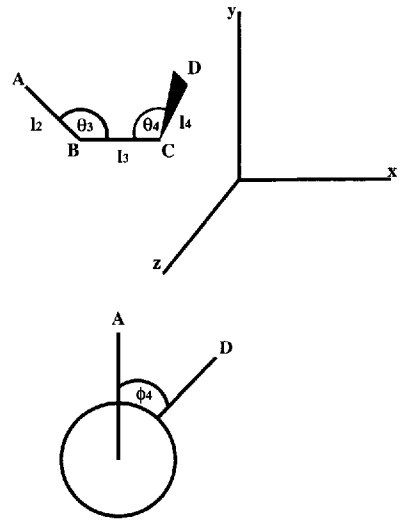

Figure 1. The definition of terms in the Z-matrix.

The cartesian coordinates of atom D on line n are generated from the following matrix equation,

$$\begin{pmatrix} x_D \\ y_D \\ z_D \end{pmatrix} = \begin{pmatrix} x_C \\ y_C \\ z_C \end{pmatrix} + \boldsymbol{A} \cdot \boldsymbol{T} \begin{pmatrix} l_n \\ 0 \\ 0 \end{pmatrix} \tag{1}$$

where $\boldsymbol{T}$ is defined in terms of the Z-matrix angles θ_n, ϕ_n,

$$\boldsymbol{T}(\theta_n, \phi_n) = \begin{pmatrix} \cos\theta_n & \sin\theta_n & 0 \\ \sin\theta_n \cos\phi_n & -\cos\theta_n \cos\phi_n & \sin\phi_n \\ \sin\theta_n \sin\phi_n & -\cos\theta_n \sin\phi_n & \cos\phi_n \end{pmatrix} \tag{2}$$

and the matrix $\boldsymbol{A}$ is defined in terms of the Euler angles θ, ϕ and ψ which rotate the cartesian axes onto the dummy axis system defined in terms of atoms A, B, C in figure 1 with atom C at the origin,

$$A(\theta,\phi,\psi)=\begin{pmatrix}\cos\phi\cos\psi-\sin\phi\cos\theta\sin\psi & \sin\phi\cos\psi+\cos\phi\cos\theta\sin\psi & \sin\theta\sin\psi\\ -\cos\phi\sin\psi-\sin\phi\cos\theta\cos\psi & -\sin\phi\sin\psi+\cos\phi\cos\theta\cos\psi & \sin\theta\cos\psi\\ \sin\phi\sin\theta & -\cos\phi\sin\theta & \cos\theta\end{pmatrix}. \quad (3)$$

In the Monte Carlo calculations random changes were made to the Z-matrix coordinates Γ using the procedure described below. The energy $U(\Gamma_m)$ of each conformation m was calculated using a modified form of the MM2 molecular mechanics force-field. The changes to the original MM2 force-field [7] involved replacing bond dipoles by equivalent partial electronic charges interacting via a distance-dependent dielectric, and replacing the out-of-plane bending equation of MM2 with an improper torsional interaction (both standard procedures in the AMBER force-field [14–16]). In the original work of Allinger, conjugated π-systems were treated by a separate program MMP2 [17, 18] which carried out a quantum mechanical VESCF calculation to obtain the relevant force-constants. However, it has now been established that conjugated π-systems can be successfully modelled using the usual MM2 potential functions [19]. In the current work a new atom type was introduced to model the aromatic carbons in the phenyl rings of 5CB, using force-constants generated to reproduce known structures of conjugated systems [6]. For 5CB, the minimum energy inter-ring torsional angle is predicted as 37·6° which is a compromise between minimum steric repulsions between ring hydrogens (when the phenyl rings are at 90° to each other), and the maximum degree of conjugation provided by coplanar rings. In setting up the initial Z-matrix for 5CB, molecular mechanics calculations were carried out to find the global minimum energy conformation. In the case of 5CB this corresponds to an all-*trans* alkyl chain. The minimum energy structure was optimised to a high tolerance ($<10^{-3}$ Å) and where minor anomalies arose between bond lengths and angles which should be equal by symmetry, these were averaged by hand to produce the Z-matrix given in table 1. For example, the bond lengths of the three terminal hydrogens were found to vary by a small amount ($\approx 4\times10^{-4}$ Å) and so were set equal to the average of the three values. The minimum energy conformation of 5CB is shown in figure 2 along with the numbering scheme used in the Z-matrix of table 1.

At each Monte Carlo step a trial geometry was generated by choosing a bond angle θ_i and a dihedral angle ϕ_j at random and making a random change to both in the range $-\theta^{max}<\theta_i<\theta^{max}$, $-\phi^{max}<\phi_j<\phi^{max}$. The energy difference between the new and old conformations, $\Delta U=U(\Gamma_{new})-U(\Gamma_{old})$, was then used to accept or reject moves by the usual Metropolis method [10]. In this work, bond lengths were kept fixed for convenience, although changes to bond lengths can easily be incorporated into this Monte Carlo scheme. For ring systems it is not possible to carry out single torsional angle rotations without severely disrupting the structure of the ring. Although such moves would normally be rejected because they generate extremely high energy conformations, it is convenient to remove such moves from the simulations altogether. In this work a rigid sub-structure for 5CB was defined by freezing the motion of certain ring dihedrals and bond angles. The constrained angles are indicated by superscript [a] in table 1. For rings which change structure via the concerted rotation about more than one dihedral angle (as in cyclohexane or tetrahydrofuran) special multi-angle Monte Carlo moves would be required in addition to single changes in the Z-matrix proposed here [20]. Strictly, when elements of the molecular structure are constrained, equilibrium should be generated with a probability proportional to $\exp(-(U/k_BT)-1/2\ln|\mathbf{H}|)$, where $|\mathbf{H}|$ is the determinant of a metric tensor which arises from setting the conjugate momenta of the constraints to zero [21]. For the bond length constraints used in this model, $|\mathbf{H}|$ is a function of all the angles in the system. However, since the angles always stay close to their equilibrium values, the influence of $|\mathbf{H}|$ is expected to be very small, changing the conformational equilibrium by $<1\%$ [21], and so has been ignored in these simulations. The constrained bond angles and

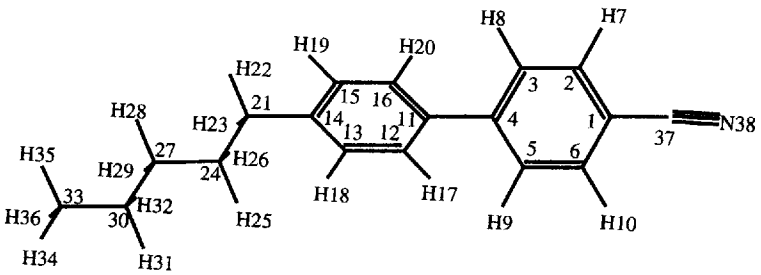

Figure 2. The minimum energy conformation for 5CB in the MM2 force-field

Table 1. Z-matrix for 5CB.

Line no.	Atom A	B	C	D	Bond length l_n	Bond angle θ_n	Dihedral angle ϕ_n
1	C11						
2	C11	C04			1·5041		
3	C11	C04	C03		1·3946	120·000	
4	C11	C04	C03	C02	1·3946	120·000[a]	180·0[a]
5	C04	C03	C02	C01	1·3946	120·000[a]	0·0[a]
6	C03	C02	C01	C06	1·3946	120·000[a]	0·0[a]
7	C02	C01	C06	C05	1·3946	120·000[a]	0·0[a]
8	C03	C02	C01	C37	1·3154	120·000[a]	180·0[a]
9	C03	C02	C01	N38	2·4795	120·000[a]	180·0[a]
10	C03	C04	C11	C16	1·3946	120·000	−37·6
11	C04	C11	C16	C15	1·3946	120·000[a]	180·0[a]
12	C11	C16	C15	C14	1·3946	120·000[a]	0·0[a]
13	C16	C15	C14	C13	1·3946	120·000[a]	0·0[a]
14	C15	C14	C13	C12	1·3946	120·000[a]	0·0[a]
15	C16	C15	C14	C21	1·5108	120·715	180·0[a]
16	C15	C14	C21	C24	1·5363	110·872	−89.9
17	C14	C21	C24	C27	1·5373	111·913	180·0
18	C21	C24	C27	C30	1·5370	111·962	180·0
19	C24	C27	C30	C33	1·5345	111·818	180·0
20	C04	C03	C02	H07	1·1038	119·405	180·0[a]
21	C11	C04	C03	H08	1·1024	120·590	0·0[a]
22	C01	C06	C05	H09	1·1024	118·411	180·0[a]
23	C02	C01	C06	H10	1·1038	120·372	180·0[a]
24	C14	C13	C12	H17	1·1024	118·424	180·0[a]
25	C15	C14	C13	H18	1·1028	119·916	180·0[a]
26	C11	C16	C15	H19	1·1028	119·418	180·0[a]
27	C04	C11	C16	H20	1·1024	120·603	0·0[a]
28	C15	C14	C21	H22	1·1153	109·728	31·9
29	C15	C14	C21	H23	1·1153	109·708	148·4
30	C14	C21	C24	H25	1·1162	109·366	−58·7
31	C14	C21	C24	H26	1·1162	109·364	58·7
32	C21	C24	C27	H28	1·1160	109·370	−58·7
33	C21	C24	C27	H29	1·1160	109·369	58·7
34	C24	C27	C30	H31	1·1164	109·585	−58·8
35	C24	C27	C30	H32	1·1164	109·586	58·8
36	C27	C30	C33	H34	1·1144	111·149	180·0
37	C27	C30	C33	H35	1·1144	111·149	−60·1
38	C27	C30	C33	H36	1·1144	111·149	60·1

[a] indicates a constrained angle.

torsions in table 1, would not normally be expected to change much in an unconstrained simulation and their influence on $|\mathbf{H}|$ is negligible.

Calculations were carried out on an HP 9000 715/75 workstation, at a rate of 140 trial moves per second. Typically, most thermodynamic properties were converged within 1×10^6 trial moves, though dihedral angle distributions required $\approx 20 \times 10^6$ to produce a smooth distribution across the entire angle range. Production runs were carried out for between $40–140 \times 10^6$ trial moves. The maximum angle displacements θ^{max}, ϕ^{max} were adjusted independently during the simulation so that the acceptance ratio for trial moves was in the region of 45–60%. For most dihedrals $50° < \phi_i^{max} < 90°$ at 300 K, with $7° < \theta^{max} < 10°$.

3. Gas phase results

In the model of 5CB used in this study, 6 dihedral angles are free to rotate. The distribution functions $S(\phi)$ for each of these angles is shown in figure 3. In figure 3 (*a*) the inter-ring torsion exhibits four-fold maxima in $S(\phi)$ as expected, with figure 3 (*b*) showing that the alkyl chain prefers to lie perpendicular to the plane of the terminal phenyl ring. $S(\phi)$ in figure 3 (*f*) corresponds to the rota-

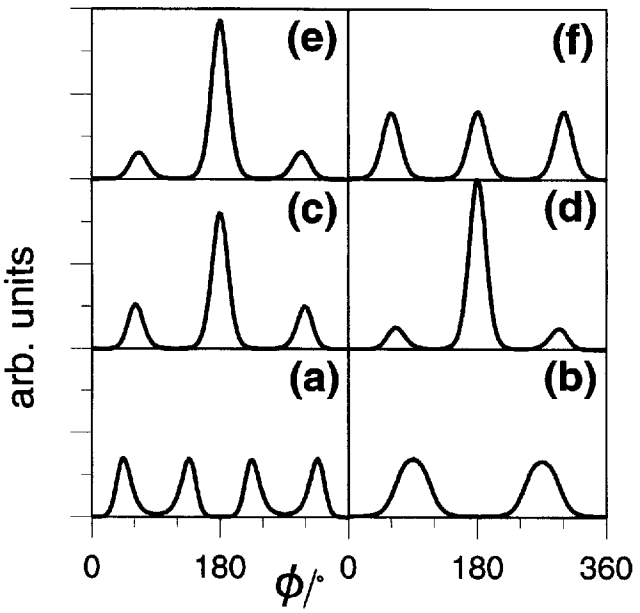

Figure 3. The dihedral angle distributions in the gas phase of 5CB at 300 K: (*a*) C5–C4–C11–C16, (*b*) C15–C14–C21–C24, (*c*) C14–C21–C24–C27, (*d*) C21–C24–C27–C30, (*e*) C24–C27–C30–C33, (*f*) C27–C30–C33–H34.

tion of the terminal methyl group about the C30–C33 bond. The almost perfect threefold symmetry here testifies to the quality of phase-space sampling provided by the Monte Carlo method. The surprise from figure 3 is provided by the unexpected ordering of *gauche/trans* populations for the three chain dihedrals C14–C21–C24–C27, C21–C24–C27–C30 and C24–C27–C30–C33. Integration and normalization of these curves (figure 3 (*c*–*e*)) provides the relative populations for *gauche*-minus, *trans* and *gauche*-plus conformers in table 2. The results indicate that *gauche* conformers are most likely for the dihedral angle C14–C21–C24–C27 nearest to the biphenyl core, and least likely for the middle dihedral C21–C24–C27–C30. Explanation of this can be found through the examination of individual energy minimized structures for *gauche* conformers of these dihedral angles. For the dihedral angle C14–C21–C24–C27 *gauche* conformers result in a molecular structure which is considerably bent and

Table 2. *Gauche-trans* populations for chain dihedral angles of 5CB in the gas phase at 300 K.

Dihedral angle	*g*−	*t*	*g*+
C14–C21–C24–C27	19·13	62·44	18·43
C21–C24–C27–C30	10·37	79·55	10·08
C24–C27–C30–C33	13·02	73·62	13·36

which is stabilised by attractive van der Waals interactions between chain atoms and atoms in the ring structure of 5CB. For long enough carbon chains it may even be possible to overcome the energy gap between *gauche* and *trans* conformers via this mechanism. In contrast, *gauche* conformers for the dihedral angle C21–C24–C27–C30 point the end of the chain away from the biphenyl rings and so favourable chain-ring interactions are minimal.

$S(\phi)$ can be written in terms of an effective torsional potential or conformational free energy $E_{\text{eff}}(\phi)$, [22],

$$S(\phi) = C \exp\left[\frac{-E_{\text{eff}}(\phi)}{k_{\text{B}}T}\right] \tag{4}$$

where C is a normalization factor. Extraction of $E_{\text{eff}}(\phi)$ from equation (4) yields the effective torsional potential curves of figure 4. From figure 4 the relative energies between *trans* and *gauche* conformations ΔE_{tg} are 2·8 kJ mol^{-1} for C14–C21–C24–C27 (at 61°, 299°), 5·2 kJ mol^{-1} for C21–C24–C27–C30 (at 66°, 295°), 4·4 kJ mol^{-1} for C24–C27–C30–C33 (at 67°, 295°), indicating that chain-ring interactions stabilize the *gauche* conformation of dihedral C14–C21–C24–C27 to the extent of $\approx$2·4 kJ mol^{-1}. One might intuitively expect that it would be easier to rotate about bonds the nearer one got to the end of the chain. Some evidence for this is provided in figure 4 from the observation that the energy barrier $\Delta E_{tg}^{\text{barrier}}$ to rotation between *trans* and *gauche* conformations drops as one goes down the alkyl

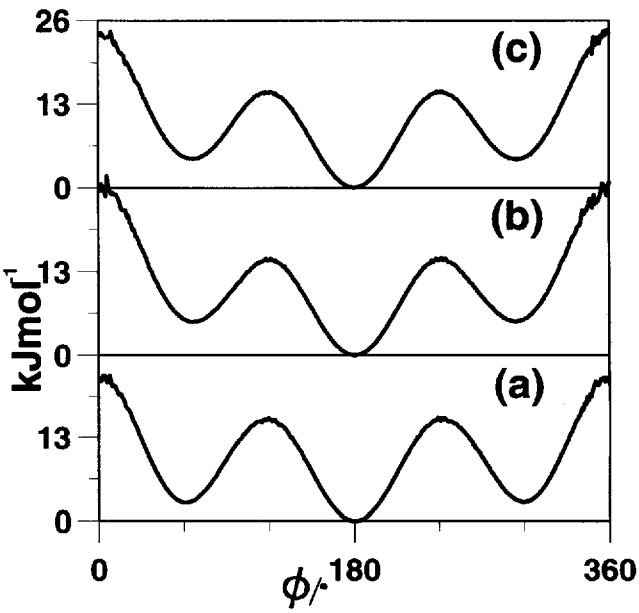

Figure 4. Effective torsional potentials in the gas phase of 5CB at 300 K: (*a*) C14–C21–C24–C27, (*b*) C21–C24–C27–C30, (*c*) C24–C27–C30–C33.

chain; $\Delta E_{tg}^{barrier} = 16{\cdot}1$, $15{\cdot}1$, $15{\cdot}0\,kJ\,mol^{-1}$, respectively for rotations about C21–C24, C24–C27 and C27–C30 bonds. It has not proved possible to calculate the *gauche–gauche* energy barrier $\Delta E_{gg}^{barrier}$ accurately because so few molecular configurations are generated in this region of phase space. It is interesting to compare these results with the rotational isomeric state model (RIS) of Flory [23], which is often used to predict the structures of liquid crystal molecules. In the simplest form of the RIS model, a single energy term is used to describe the change in internal energy caused by any *gauche* conformation regardless of its position in the alkyl chain. The results of this work suggest that this assumption is dubious.

From the simulations it is possible to extract the relative populations of individual conformation of 5CB in the gas phase. In table 3, chain conformational populations have the preferred order, $ttt > gtt > ttg > tgt$. Although the all-*trans* chain is favoured, the relative effect of the chain–core van der Waals interactions discussed above is to favour *gauche* conformers which lead to an overall bent molecular shape. This is the opposite of what one would expect for liquid crystal molecules in a condensed phase. In the nematic phase, the anisotropic nature of molecular interactions mean that molecules exist in an ellipsoidal cavity within the fluid, so one would normally expect more elongated conformers (*tgt*) to be favoured. To examine the validity of this assumption, § 4 investigates the effect of coupling the molecular structure to a nematic mean field via a conformationally dependent potential of mean torque.

4. The effect of a nematic mean field

Following Emsley, Luckhurst and Stockley (ELS), the energy of a molecule in a nematic mean field can be written as [24],

$$U(\Gamma, \omega) = U_{int}(\Gamma) + U_{ext}(\Gamma, \omega) \qquad (5)$$

where $U_{int}(\Gamma)$ is the conformational internal energy, and $U_{ext}(\Gamma, \omega)$ is the potential of mean torque for a molecule in orientation ω and conformation described by the internal coordinates Γ. In the work of ELS, U_{int} is described by the (RIS) model, and is considered to be independent of molecular orientation. This means that energy barriers to rotation are uninfluenced by the orientation of the molecule. In the current work U_{int} is simply equated to the energy of a molecule in the MM2 force-field (as in § 2).

Table 3. Conformational populations for 5CB in the gas phase at 300 K.

Dihedral C14–C21–C24–C27	Dihedral C21–C24–C27–C30	Dihedral C24–C27–C30–C33	%
$g-$	$g-$	$g-$	0·27
$g-$	$g-$	t	2·01
$g-$	$g-$	$g+$	0·02
$g-$	t	$g-$	2·73
$g-$	t	t	11·45
$g-$	t	$g+$	2·03
$g-$	$g+$	$g-$	0·00
$g-$	$g+$	t	0·44
$g-$	$g+$	$g+$	0·08
t	$g-$	$g-$	1·25
t	$g-$	t	6·13
t	$g-$	$g+$	0·13
t	t	$g-$	6·70
t	t	t	33·72
t	t	$g+$	7·02
t	$g+$	$g-$	0·13
t	$g+$	t	6·20
t	$g+$	$g+$	1·25
$g+$	$g-$	$g-$	0·07
$g+$	$g-$	t	0·45
$g+$	$g-$	$g+$	0·00
$g+$	t	$g-$	1·81
$g+$	t	t	11·51
$g+$	t	$g+$	2·50
$g+$	$g+$	$g-$	0·02
$g+$	$g+$	t	1·79
$g+$	$g+$	$g+$	0·29

Expanding $U_{ext}(\Gamma, \omega)$ in modified spherical harmonics $C_{L,m}$ [25] yields,

$$U_{ext}(\Gamma, \beta\gamma) = -\sum_{L,m}{}' (-)^m \varepsilon_{L,m} C_{L,-m}(\beta\gamma), \qquad (6)$$

where $\varepsilon_{L,m}$ is an interaction tensor written in irreducible form, β, γ are spherical polar angles of the director in the molecular coordinate system and the prime denotes that only even terms in the expansion have been kept. Truncating the expansion at $L = 2$ and working in the principal axis system of the interaction tensor, allows $U_{ext}(\Gamma, \beta\gamma)$ to be written as [25],

$$U_{ext}(\Gamma, \beta\gamma) = -\varepsilon_{2,0} P_2(\cos\beta) - \varepsilon_{2,2}\left(\frac{3}{2}\right)^{1/2} \sin^2\beta \cos 2\gamma \qquad (7)$$

where the $\varepsilon_{2,0}$ and $\varepsilon_{2,2}$ can be related to the cartesian components of the interaction tensor by,

$$\varepsilon_{2,0} = \left(\frac{2}{3}\right)^{1/2}\left(\varepsilon_{zz} - \frac{\varepsilon_{xx} - \varepsilon_{yy}}{2}\right)$$
$$\varepsilon_{2,2} = \frac{\varepsilon_{xx} - \varepsilon_{yy}}{2}. \qquad (8)$$

In the work of ELS [24, 25], an explicit expression for $\varepsilon_{L,m}(\Gamma)$ is derived in terms of two variables X_a and X_c which, respectively, represent the interaction of the whole core and chain C–C bonds with the nematic mean field. X_a and X_c and the *trans-gauche* energy terms in the RIS representation can then be optimised to provide good fits with data derived from NMR experiments. The current work is mainly concerned with providing a generalized scheme for predicting the structures of mesogenic molecules, and so a slightly simpler form for $U_{ext}(\Gamma, \beta\gamma)$ has been taken below. This form can immediately be used to provide first predictions of the structures of mesogens without the prior need for detailed NMR data. The current scheme could easily be modified along the lines of the ELS model, though such a modification would require lengthy simulations to provide the correct values of X_a and X_c for a given molecule at a given temperature.

Equation (7) requires that molecular shape should be coupled in some way to the potential of mean torque. A convenient way of doing this is by linking U_{ext} to the moment of inertia tensor. The latter is defined by

$$I_{\alpha\beta}(\Gamma) = \sum_i m_i(r_i^2 \delta_{\alpha\beta} - r_{i\alpha} r_{i\beta}),$$
$$\alpha, \beta = x, y, z; \qquad (9)$$

where m_i is the mass of atom i and the atomic positions r_i are measured relative to the centre of mass. Diagonalization of $\mathbf{I}(\Gamma)$ yields three eigenvalues corresponding to the principal moments of inertia I_{aa}, I_{bb} and I_{cc} together with three eigenvectors **a**, **b** and **c** giving the principal molecular axes. The values can then be used to construct an equivalent inertia spheroid for a molecule. This spheroid is defined to have uniform mass density and have the same moments of inertia and the same total mass M as the molecule under investigation, and has semi-axis lengths given by a, b, c where $a(\Gamma) = (2{\cdot}5(I_{bb} + I_{cc} - I_{aa})/M)^{1/2}$ (with cyclic permutations for $b(\Gamma)$ and $c(\Gamma)$). The inertia spheroid can be used in equation (7) by equating the values of a, b, c to the cartesian components of the interaction tensor. In doing this, it is assumed that the principal axis system of the interaction tensor coincides with that of the inertia tensor. As a first approximation the biaxial term in the equation for U_{ext} has been ignored. Accordingly, U_{ext} is written as,

$$U_{ext} = -v\xi(\Gamma) P_2(\cos\beta), \qquad (10)$$

where $\xi(\Gamma) = a(\Gamma) - (b(\Gamma) + c(\Gamma))/2$ and v is a measure of the strength of the potential of mean torque. In the simplest form of the Maier–Saupe mean field theory [26], v is proportional to the average value of the order parameter $\langle P_2(\cos\beta)\rangle$. Here, $\langle P_2(\cos\beta)\rangle$ is determined from the calculations at fixed v and temperature T. The neglect of molecular biaxiality in formulating U_{ext} simplifies the Monte Carlo simulations, but represents a rather coarse approximation. Although biaxial contributions to the total energy tend to be small, their influence can be significant. In the current scheme a biaxial term (proportional to $c(\Gamma) - b(\Gamma)$) could be added to U_{ext}. However, this would require an additional unknown constant to be fixed by comparison with the experimental biaxial order parameter. In this work, the simpler form for U_{ext}, in equation (7), greatly reduces the amount of computation required.

For convenience the director is fixed during the simulations along the z-axis of space and molecules are allowed to rotate under the constraints of U_{ext}. At each step diagonalization of $\mathbf{I}(\Gamma)$ yields β, $a(\Gamma)$, $b(\Gamma)$, $c(\Gamma)$ and consequently U_{ext}. The following matrix equation was used to specify the atomic coordinates,

$$\begin{pmatrix} x'_D \\ y'_D \\ z'_D \end{pmatrix} = \boldsymbol{Q} \cdot \begin{pmatrix} x_D \\ y_D \\ z_D \end{pmatrix} \qquad (11)$$

where the vector (x_D, y_D, z_D) was generated from equation (1) and

$$\boldsymbol{Q}=\begin{pmatrix} q_0^2+q_1^2-q_2^2-q_3^2 & 2(q_1q_2+q_0q_3) & 2(q_1q_3-q_0q_2) \\ 2(q_1q_2-q_0q_3) & q_0^2-q_1^2+q_2^2-q_3^2 & 2(q_2q_3+q_0q_1) \\ 2(q_1q_3+q_0q_2) & 2(q_2q_3-q_0q_1) & q_0^2-q_1^2-q_2^2+q_3^2 \end{pmatrix}. \tag{12}$$

In equation (12), q_0, q_1, q_2 and q_3 are the quarternions,

$$\begin{aligned} q_0 &= \cos\frac{1}{2}\theta\cos\frac{1}{2}(\phi+\psi) \\ q_1 &= \sin\frac{1}{2}\theta\cos\frac{1}{2}(\phi-\psi) \\ q_2 &= \sin\frac{1}{2}\theta\sin\frac{1}{2}(\phi-\psi) \\ q_3 &= \cos\frac{1}{2}\theta\sin\frac{1}{2}(\phi+\psi) \end{aligned} \tag{13}$$

which specify the orientation of the first bond in the Z-matrix in terms of its Euler angles θ,ϕ,ψ relative to the cartesian axes x,y,z [10].

Monte Carlo trial moves consisted of a combined conformational/rotational move, with the conformational change handled in the manner described in § 2, and the rotational part of the move handled using the method described by Vesely [27]. The change in energy at each step is computed from equations (5) and (7). After adjusting the sizes of θ^{max},ϕ^{max} (as in § 2), the maximum size of rotational moves was adjusted to give an overall acceptance rate of between 40–50%.

5. Mean field results

Monte Carlo simulations were carried out for 9 values of the mean field strength v in the range 0–2·0 kJ mol^{-1} Å^{-1}. The results from these simulations are summarized in table 4. The potential of mean torque in equation (7) is found to have a significant influence on the overall shape of 5CB. This is witnessed in the changing values of the length, width and breadth $(2a,2b,2c)$ of the equivalent moment of inertia spheroid in table 4. These results are of course expected from the form used for U_{ext} in this model, but it is worth noting that they are similar to the results found by Wilson and Allen in their simulations of 128 molecules of 4-(*trans*-4-*n*-pentylcyclohexyl)cyclohexylcarbonitrile (CCH5) in the bulk nematic phase [22, 28].

In a nematic phase, the effective torsional free energy of equation (4) can be written as [29],

$$E_{eff}(\phi)=E_{nem}(\phi)+E(\phi)_{torsion}, \tag{14}$$

where E_{nem} is the contribution to $E_{eff}(\phi)$ from the nematic field and $E(\phi)_{torsion}$ is the rotational potential in the gas phase. In figure 5, E_{nem} is plotted for different mean field strengths v for the three chain torsional angles. The nematic field has a dramatic influence on the first dihedral angle in the chain (C14–C21–C24–C27), and rotational trial moves away from $\phi=180°$ become increasingly high in energy as the field strength is turned up. E_{nem} is well fit by a quartic polynomial, though statistics are rather poor at the *gauche-gauche* energy barrier. The form of E_{nem} in figure 5 is similar to that seen by Cross and Fung in their simulations of 5CB in the bulk nematic phase, though the magnitude of E_{nem} is slightly higher in their work for similar core order parameters. The influence of E_{nem} on the two other dihedrals in the chain (C21–C24–C27–C30 and C24–C27–C30–C33) is rather smaller than that seen for C14–C21–C24–C27. This reflects the fact that changes in these two dihedrals influence molecular shape much less than changes to C14–C21–C24–C27. At high mean fields, the overall effect of E_{nem} is to reduce the *trans-gauche* energy gap for rotations about C24–C27 and to increase it very slightly for rotations about C27–C30. The result of these changes to E_{eff} is reflected in table 5 which lists the relative populations of different chain conformers as a function of v. The all-*trans* conformation

Table 4. Simulation data for 5CB under the application of a potential of mean torque $U_{ext}(\Gamma,\beta\gamma)$ at 300 K.

v/kJ mol^{-1} Å^{-1}	$\langle U\rangle$/kJ mol^{-1}	$\langle U_{ext}\rangle$/kJ mol^{-1}	$\langle P_2\rangle$	$\langle P_2\rangle_{core}$ (C_1–C_{14})	$\langle a\rangle$/Å	$\langle b\rangle$/Å	$\langle c\rangle$/Å
0·00	99·44	0·00	0·00	0·00	9·42	2·32	1·470
0·50	98·04	−1·29	0·34	0·32	9·47	2·30	1·460
0·75	96·54	−2·83	0·49	0·46	9·49	2·27	1·453
0·875	95·56	−3·75	0·56	0·53	9·51	2·26	1·450
1·00	94·54	−4·73	0·61	0·58	9·53	2·25	1·443
1·25	92·54	−6·77	0·70	0·66	9·57	2·23	1·437
1·50	90·35	−8·84	0·76	0·72	9·60	2·21	1·425
1·75	88·18	−10·93	0·80	0·76	9·64	2·19	1·410
2·00	86·10	−13·01	0·83	0·79	9·66	2·17	1·405

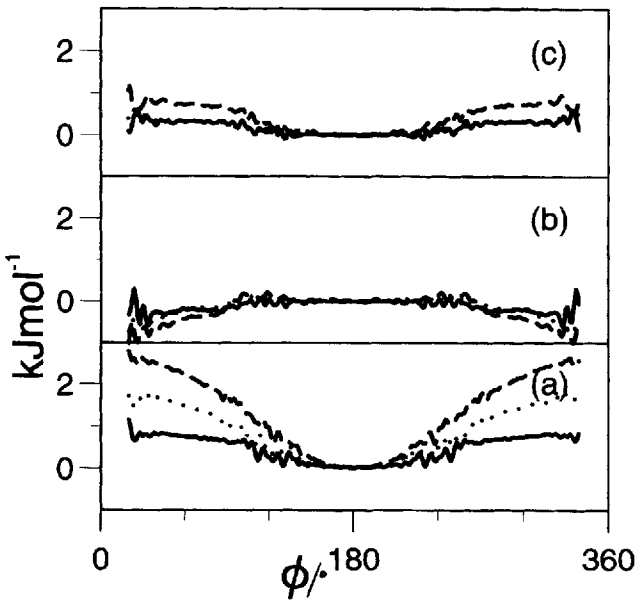

Figure 5. Nematic contributions (E_{nem}) to the effective torsional potentials for 5CB under the application of a potential of mean torque $U(\Gamma, \beta\gamma)$. Drawn line $v = 0{\cdot}75\,kJ\,mol^{-1}\,Å^{-1}$; dotted line $v = 1{\cdot}25\,kJ\,mol^{-1}\,Å^{-1}$; dashed line $v = 1{\cdot}75\,kJ\,mol^{-1}\,Å^{-1}$. (*a*) C14–C21–C24–C27, (*b*) C21–C24–C27–C30, (*c*) C24–C27–C30–C33.

Table 5. Conformational populations for chain dihedral angles under the application of a potential of mean torque $U_{ext}(\Gamma, \beta\gamma)$ at 300 K.

v / kJ mol^{-1} Å^{-1}	*ttt*/%	*gtt*/%	*tgt*/%	*ttg*/%
0·00	32·72 ± 0·14	23·0 ± 0·3	12·3 ± 0·2	13·7 ± 0·2
0·50	36·7 ± 0·4	20·9 ± 0·7	13·7 ± 0·6	13·1 ± 0·4
0·75	38·2 ± 2·7	19·2 ± 0·8	14·4 ± 0·4	13·3 ± 0·4
0·875	39·0 ± 2·0	18·4 ± 0·9	14·5 ± 0·6	13·7 ± 0·6
1·00	40·1 ± 0·5	17·6 ± 0·8	14·9 ± 0·6	14·0 ± 0·6
1·25	42·3 ± 1·6	15·3 ± 0·8	15·3 ± 0·6	14·0 ± 0·8
1·50	43·4 ± 1·3	14·5 ± 0·6	16·5 ± 0·7	13·8 ± 0·4
1·75	46·1 ± 1·0	12·5 ± 0·6	17·6 ± 0·5	13·2 ± 0·6
2·00	47·6 ± 0·9	11·7 ± 0·4	17·5 ± 0·9	13·8 ± 0·6

is significantly enhanced by the application of the mean field with the all-*trans* population reaching a value of 47·6% at $v = 2{\cdot}0\,kJ\,mol^{-1}\,Å^{-1}$ which corresponds to a core order parameter of 0·79. The preference for *gtt* as the favoured *gauche* chain conformation (stabilized by ring-chain interactions in the gas phase) is removed, as mean field strength is increased. As v increases the preferred chain *gauche* conformation becomes the *tgt* conformation which is the most linear of the *gauche* conformations and therefore makes the largest contribution to ξ. As in bulk simulations of 5CB [29, 30] and CCH5 [22], the overall effect of the nematic field is to favour those conformations where bonds lie along the molecular long-axis. So the preferred order of chain conformations is *ttt* > *tgt* > *ttg* > *gtt* at high values of v, and is significantly different from the gas phase results of § 3. It is worth noting however, that it is only when v reaches a value of $1{\cdot}25\,kJ\,mol^{-1}\,Å^{-1}$ that the *tgt* conformer becomes favoured over *gtt*. This order for chain conformers also occurs in simulations of the liquid phase of CCH5 [22], and therefore suggests that the simple form of the potential of mean torque used in equation (7) does not fully take into account the changes in structure between the fluid and gas phases. This is not altogether surprising. Anisotropic molecules exist in an ellipsoidal cavity even in the liquid phase, and an additional term could be added to equation (7) to take this into account. Samulski and Dong [31] have suggested a model where a molecule is enclosed inside a hypothetical (penetrable) cylinder with the cylinder axis coincident with the vector **a** of § 4, and each atom interacting with the nearest point on the cylinder via a Lennard–Jones potential. Whilst this potential could be added directly to equation (7), it would again prove difficult to calibrate a general form of the potential which would be suitable for use with any liquid crystal molecule.

Finally, it is interesting to compare the predictions of this model with experimental evidence of molecular shape provided by NMR investigations. Deuterium NMR studies have been carried out for 5CB by Emsley *et al.* [32], and values of the quadrupolar couplings $\tilde{q}$ are available for the alkyl chain at 300 K. Assuming that the quadrupolar tensor for a deuteron is cylindrically symmetric about the C–D bond, then the quadrupolar coupling for position k in the chain can be written as,

$$\tilde{q}_k = q_{CD} S_{CD_k} \tag{15}$$

where q_{CD} is the component of the quadrupolar tensor along the C–D bond and S_{CD_k} is the order parameter for the bond. S_{CD_k} is calculated directly in the simulations as,

$$S_{CD_k} = \langle P_2(\cos(\mathbf{n} \cdot \hat{\mathbf{r}}_{CD})) \rangle \tag{16}$$

where $\hat{\mathbf{r}}_{CD}$ is the unit vector along the C–D bond. In table 6 there are included values of S_{CD_k} calculated from the simulations for different positions in the alkyl chain as a function of v. NMR values of S_{CD_k} are also included in table 6, using the assumption that q_{CD} is independent of position in the alkyl chain. The trend in the values of S_{CD_k} is correctly predicted by the simulations, in particular the drop in $|S_{CD_k}|$ in going from $k = 4$ to $k = 5$, which is not seen if U_{ext} is taken to be independent of conformational state [32]. Using the data of Emsley *et al.* for an axis fixed in the ring adjacent to the cyano group, $\langle P_2 \rangle$ (at 300 K) can be estimated to be 0·545. This is most closely matched by the simulations at $v = 0{\cdot}875\,kJ\,mol^{-1}\,Å^{-1}$ ($\langle P_2 \rangle = 0{\cdot}53$) $v = 1{\cdot}0\,kJ\,mol^{-1}\,Å^{-1}$

Table 6. Order parameters for C–H(D) bonds in the aromatic core and the alkyl chain of 5CB for different mean field strengths at 300 K. 'Core' indicates the mean of bond order parameters in the aromatic core. 'Chain 1' indicates the chain bond nearest the aromatic core. NMR order parameters are derived (from data in reference [32]) by using values of 168 and 185 kHz for the quadrupolar coupling constant for the alkyl chain and aromatic ring deuterons, respectively.

v/kJ mol^{-1} Å^{-1}	Core	Chain 1	Chain 2	Chain 3	Chain 4	Chain 5
0·5	−0·047	−0·136	−0·068	−0·071	−0·046	−0·031
0·75	−0·067	−0·195	−0·107	−0·107	−0·065	−0·047
0·875	−0·078	−0·223	−0·125	−0·127	−0·083	−0·057
1·00	−0·084	−0·243	−0·147	−0·148	−0·094	−0·068
1·25	−0·096	−0·276	−0·163	−0·168	−0·109	−0·077
1·50	−0·104	−0·301	−0·196	−0·198	−0·131	−0·901
1·75	−0·110	−0·318	−0·211	−0·212	−0·149	−0·104
2·00	−0·114	−0·329	−0·231	−0·234	−0·161	−0·113
NMR	−0·044	−0·202	−0·137	−0·147	−0·099	−0·072

($\langle P_2 \rangle = 0{\cdot}58$). The predicted order parameters from these simulations are quite close to the experimental values, though the theoretical results rather over-predict the values of $|S_{CD}|$ for the C–D bond closest to the core, and the C–D bonds in the aromatic core itself. This may be a function of the simplified form taken for U_{ext} in equation (7), where the influence of molecular biaxiality on core and chain has been neglected, or may simply reflect the neglect of short-range intermolecular forces in the model (as discussed above). The latter would be expected to increase the ordering of the chain (through quenching out of the *gauche* conformers *gtt*, *ttg*). A more ordered chain would lead to the matching of experimental and theoretical order parameters (for the ring adjacent to the cyano group) at a lower value of v. This in turn would lead to lower predicted values of S_{CD} for C–D bonds in the core, and for the first carbon in the chain, together with higher values of S_{CD} for C–D bonds further down chain.

6. Conclusions

The Monte Carlo method introduced here provides excellent statistics for dihedral distribution functions and conformational averages for the expenditure of modest amounts of computer time. In comparison, trial stochastic dynamics simulations for 5CB using the same force-field and the van Gunsteren/Berendsen method [11] provided very poor statistics at 300 K for even long runs in excess of 10 ns. Work by Guarnieri and Still on a 5 site united atom model of pentane at 300 K has recently indicated that average dihedral angle distributions had not fully converged even after runs in excess of 1 μs [12]. Such run lengths are currently out of the question for large liquid crystal molecules.

The gas phase structures of 5CB show that the alkyl chain prefers an all-*trans* configuration but that the *gtt* conformer is chosen in preference to *ttg* and *tgt*. The overall conformer order of $ttt > gtt > ttg > tgt$ occurs because favourable chain/core interactions are maximized when the alkyl chain is allowed to *curl up* on itself. However, the application of a conformationally dependent potential of mean torque U_{ext} causes elongated conformers to become favoured, and changes the preferred conformer order to $ttt > tgt > ttg > gtt$. The influence of the nematic field is something which is largely (and incorrectly) ignored in most molecular mechanics (MM) studies of mesogens. The approach adopted here provides a general and simple mechanism to improve upon mesogenic structures predicted from traditional MM studies.

Comparison of data from this study with experimental deuterium NMR work suggests that the number of *gtt* (and to a lesser extent *ttg*) conformers predicted for 5CB may still be too large. This may be due to an over-preference for the *gtt* conformer caused by the MM2 force-field, or simply from the use of an over-simplified form for U_{ext}. It should also be stressed that the use of a mean field for U_{ext} is unlikely to take fully into account the effects of intermolecular interactions with neighbouring molecules in the fluid. 5CB molecules exist in an elliptical cavity formed from surrounding molecules in both the liquid and the nematic phase, and this cavity is difficult to model accurately within a one molecule model.

Several adaptations of the current work are possible. The integration over angles ω, considered in § 4, can be carried out directly for each configuration Γ. This has been considered in recent work by Ferrarini, Luckhurst and Nordio [33], and provides a possible alternative to the Monte Carlo approach advocated in the current study. The addition of the biaxiality term in equation (7) and/or further terms in the expansion of equation (6) are also possible, and provides a useful means of providing a more detailed form for U_{ext}. Alternatively, the Emsley, Luckhurst, Stockley model [24] may be used to provide a more sophisticated form for U_{ext}, and has been shown to give good agreement with deuterium NMR for 5CB and 8CB [24, 34]. However, in the case

of the ELS model, it is difficult to adapt this form for U_{ext} to molecules without a well-defined core structure. Ferrarini *et al.* [35] have recently suggested that U_{ext} may be written in the form,

$$U_{ext} = v \int_S P_2 \cos \psi_{\mathbf{n}_s} dS \qquad (17)$$

where $\psi_{\mathbf{n}_s}$ is the angle between the director and a vector normal to the molecular surface $\mathbf{n}_s$, and the integral is taken over all points on the surface S. Using van der Waals spheres to define the molecular surface allows U_{ext} to be defined for any geometry, with v acting as a measure of the strength of the orientational interaction (as in this work). This form for U_{ext} is computationally expensive compared to the model used here, but may provide a better measure of the U_{ext} than equation (7). Finally, the first bulk computer simulations of nematics are starting to appear in the literature [22, 28–30]. Currently such studies are very expensive, but may in the future provide detailed forms for U_{ext}.

The author would like to thank the UK EPSRC for grants towards the purchase of high-powered workstations and for travel grants through Collaborative Computational Project no. 5. Valuable discussions with Prof D. A. Dunmur and Dr M. Grayson (University of Sheffield) are gratefully acknowledged.

References

[1] Boyd, D. B., 1990, *Reviews in Computational Chemistry*, edited by K. B. Lipkowitz and D. B. Boyd (New York: VCH), Chap. 9.
[2] Allinger, N. L., 1976, *Rev. phys. org. Chem.*, **13**, 1.
[3] Burkert, O., and Allinger, N. L., 1982, *ACS Monograph*, **177** (Washington: American Chemical Society).
[4] Boyd, D. B., and Lipkowitz, K. B., 1982, *J. chem. Education*, **59**, 269.
[5] Wilson, M. R., 1988, *PhD. thesis*, University of Sheffield, Chap. 1.
[6] MacroModel V3.5X, Interactive Molecular Modelling System, 1992, Department of Chemistry, Columbia University, New York.
[7] Quantum Chemistry Program Exchange 423, 1980, MM2: *Molecular Mechanics* II (CDC Version of QCPE 395), modified by S. Profeta Jr. from the original program by N. L. Allinger and Y. H. Yuh.
[8] Stewart, J. J. P., 1990, *J. Comput. Aided Molec. Design*, **4**, 1.
[9] Dunmur, D. A., Grayson, M., and Roy, S. K., 1994, *Liq. Cryst.*, **16**, 95.
[10] Allen, M. P., and Tildesley, D. J., 1987, *Computer Simulation of Liquids* (Oxford: Oxford University Press).
[11] van Gunsteren, W. F., and Berendsen, H. J. C., 1988, *Molec. Simulation*, **1**, 173.
[12] Guarnieri, F., and Still, W. C., 1994, *J. comput. Chem.*, **15**, 1302.
[13] Clark, T., 1985, *A Handbook of Computational Chemistry: A Practical Guide to Chemical Structure and Energy Calculations* (New York: Wiley-Interscience), Chap. 3 and Appendix A.
[14] Singh, U. C., Weiner, P. K., Caldwell, J., and Kollman, P. A., 1987, *AMBER 3.0*, University of California.
[15] Weiner, S. J., Kollman, P. A., Nguyen, D. T., and Case, D. A., 1986, *J. Comput. Chem.*, **7**, 230.
[16] Weiner, S. J., Kollman, P. A., Case, D. A., Singh, U. C., Ghio, C., Alagona, G., Profeta, S., and Weiner, P., 1984, *J. Am. chem. Soc.*, **106**, 765.
[17] Allinger, N. L., and Sprague, J. P., 1973, *J. Am. chem. Soc.*, **95**, 3893.
[18] Kao, J., and Allinger, N. L., 1977, *J. Am. chem. Soc.*, **99**, 975.
[19] Wilson, M. R., 1988, *PhD. thesis*, University of Sheffield, Chap. 3.
[20] Chandrasekhar, J., and Jorgensen, W. L., 1982, *J. chem. Phys.*, **77**, 5073.
[21] Leggetter, S., and Tildesley, D. J., 1989, *Molec. Phys.*, **68**, 519.
[22] Wilson, M. R., and Allen, M. P., 1992, *Liq. Cryst.*, **12**, 157.
[23] Flory, P. J., 1969, *Statistical Mechanics of Chain Molecules* (New York: Interscience).
[24] Emsley, J. W., Luckhurst, G. R., and Stockley, C. P., 1982, *Proc. R. Soc. Lond. A.*, **381**, 139.
[25] Luckhurst, G. R., 1985, *Nuclear Magnetic Resonance of Liquid Crystals*, edited by J. W. Emsley (Dordrecht: D. Reidel), Chap. 3.
[26] Wojtowicz, P. J., 1979, *Introduction to Liquid Crystals*, edited by E. B. Priestley, P. J. Wojtowicz, and P. Sheng (New York: Plenum Press), Chap. 3.
[27] Vesely, F. J., 1982, *J. comput. Phys.*, **47**, 291.
[28] Wilson, M. R., and Allen, M. P., 1991, *Molec. Cryst. liq. Cryst.*, **198**, 465.
[29] Cross, C. W., and Fung, B. M., 1994, *J. chem. Phys.*, **101**, 6839.
[30] Komolkin, A. V., Laaksonen, A., and Maliniak, A., 1994, *J. chem. Phys.*, **101**, 4103.
[31] Samulski, E. T., and Dong, R., 1982, *J. chem. Phys.*, **77**, 5090.
[32] Emsley, J. W., Luckhurst, G. R., and Stockley, C. P., 1981, *Molec. Phys.*, **44**, 565.
[33] Ferrarini, A., Luckhurst, G. R., and Nordio, P. L., 1995, *Molec. Phys.*, **85**, 131.
[34] Counsell, C. J. R., Emsley, J. W., Heaton, N. J., and Luckhurst, G. R., 1985, *Molec. Phys.* **54**, 847.
[35] Ferrarini, A., Moro, G. J., Nordio, P. L., and Luckhurst, G. R., 1992, *Molec. Phys.*, **77**, 1.